Poly(vinyl chloride)/Metallic Oxides/Organically Modified Montmorillonite Nanocomposites: Fire and Smoke Behavior

Antonio Rodolfo, Jr.,[1,2] Lucia Helena Innocentini Mei[2]

[1]*Braskem S/A, Polymers Business Unit, Avenida das Nações Unidas, 8501, 23rd Floor, CEP 05425-070, São Paulo, SP, Brazil*
[2]*State University of Campinas, Department of Polymer Technology, School of Chemical Engineering, P. O. Box 6066, CEP 13083-970, Campinas, SP, Brazil*

Received 16 September 2009; accepted 19 October 2009
DOI 10.1002/app.31625
Published online 10 December 2009 in Wiley InterScience (www.interscience.wiley.com).

ABSTRACT: Nanocomposites of poly(vinyl chloride), metallic oxides (copper, molybdenum, and zinc), and organically modified montmorillonite (O-MMT) were prepared in a melt-blending or intercalation-in-the-molten state process, and their morphology was assessed with X-ray diffraction and transmission electron microscopy. The formation of an intercalated/partially exfoliated hybrid microstructure was confirmed in every situation studied. The combustion and smoke emission properties were studied with cone calorimetry, limiting oxygen index, and thermogravimetry (TG) coupled with mass spectroscopy (MS). The results reveal that the metallic oxides had a significant effect on both the combustion properties and smoke suppression, whereas O-MMT only affected these properties discretely. Little interaction was observed in the joint use of these additives. The results also confirm the anticipation of dehydrochlorination, reductive coupling, and benzene suppression mechanisms resulting from the presence of copper, molybdenum, and zinc metals; these were indicated by the increase in carbonaceous char residue and the significant reduction in benzene formation, in this case indicated in the TG/MS measurements obtained. © 2009 Wiley Periodicals, Inc. J Appl Polym Sci 116: 946–958, 2010

Key words: clay; flame retardance; nanocomposites; poly(vinyl chloride) (PVC)

INTRODUCTION

Since its discovery, humans have been exposed to the risks that fire provides to its users.[1] Bourbigot et al.[2] pointed out that fires, conflicts, and epidemics have always been considered the main attacks against the integrity of the human race. Because of the urban design of old cities, with high-density domiciles and an abundant use of highly flammable materials, especially wood and other natural fibers, there have been several examples of their destruction by fire, such as Rome in 64 AD, London in 1666, and even San Francisco in 1906.

With the accelerated development of mankind in the 20th century, domiciles are more equipped, with a large number of combustible materials in them, such as furniture, carpets, coverings, and the most diverse electronic devices. In the same way, industry and commerce have a larger number of goods produced and stored at the same site, and many times are surrounded by greater concentration of people in increasingly more vertical cities. In addition, new technologies are made available daily in the market, with new fire risk potential or new materials about which we do not have full knowledge.

To minimize the risks of the fire, the development of new materials resistant to combustion can be an important alternative to protect against human life loss and civil construction, such as hospitals, industries, houses, schools, libraries, and shopping centers.[3]

All organic polymers, including poly(vinyl chloride) (PVC), are combustible. When a sufficient amount of heat is supplied to any organic polymer, it decomposes thermally and can cause death by asphyxia.[4,5] In reality, the risk to life of a specific material or component under fire is a result of the combination of both flammability and the toxicity of gases released during its combustion[6] and the rate at which these toxic gases are released.[7] Other risks inherent to a fire situation are the convective and radiant heat and the low concentration of oxygen in the atmosphere; these cause a narcotic effect by the combination of a high concentration of carbon monoxide with a low concentration of oxygen. These are the most important incapacitating factors for those trying to escape a place on fire.[8]

Correspondence to: A. Rodolfo, Jr. (antonio.rodolfo@braskem.com.br).

The presence of chlorine in PVC's chemical structure provides the benefits of low flammability in products made with this polymer, but it also promotes a particular combustion mechanism that ends up generating a great amount of dense and dark smoke. This smoke is another important incapacitating factor when one analyzes a specific fire condition;[5] therefore, controlling smoke emitted by PVC compounds is very important, and it is only achieved by the addition of smoke-suppressing agents. Several smoke-suppressing agents, including zinc, boron, tin, iron, and molybdenum compounds are commercially available.[9]

Over the past decades, with the development of nanotechnology, there has been growth and, thus, increasing interest in the field of nanocomposites because of their special properties: not only because they allow one to obtain properties equivalent to traditional composites but also because they have unique optical, electrical, and magnetic properties.[10] Polymer nanocomposites have superior mechanical and chemical properties over conventional composites even with a smaller amount of reinforcement because of the greater contact area between the polymer and the dispersed phase. Furthermore, the high aspect ratio of incorporated reinforcements often provides important barrier properties. Low permeability, improved chemical resistance, and greater flame retardance are attributed to the improved barrier properties of nanocomposites. How to achieve such a performance consists of the ability to individually disperse particles with high aspect ratios in the polymer matrix.[11,12]

Polymer/clay nanocomposites are becoming a well-established area of research.[13–15] One of the most promising nanocomposite systems is those composites based on organic polymers and inorganic silicate clay minerals. PVC is a very important industrial thermoplastic, especially in applications that involve civil construction, such as finishing profiles and electric wire and cable insulation coatings, to mention just two examples. In these applications, the products are subject to increasingly stricter technical regulations and standards regarding their behavior in fire situations, regardless of the type of material used in their manufacturing.[3] The specifications cover issues directly related to material flammability, smoke production, and release of gases during combustion.

In particular, electrical cables always present a risk of fire because they often run through ducts that frequently cross through different compartments of a building and are installed in remote sites that hinder the access of people.[16] For this reason, the improved performance of those materials used as insulation in electrical wires and cables is important for the safety of building and the people who work or live in them.

Because of their chemical composition, PVC products are subject to characteristic behavior during combustion and release HCl and dense smoke. The search for new formulations and additives that alter the kinetics, or even suppress the release of these components, is very important from an academic and technological perspective, with immediate industrial applications.

Recently, nanotechnology has given special attention to the academic and industrial areas around the world, and it is considered an agent that can promote new achievements and discoveries that will certainly cause profound changes in our society. Industrial applications are increasingly gaining market share.[17] Even in the flame-retardance and smoke-suppression fields, nanotechnology stands out as a very important technological trend,[1,18] although still in an exploration process, including diverse studies with PVC as the polymeric matrix.[19–26]

Smoke suppressors in PVC, based on molybdenum and copper, were previously studied by Starnes and coworkers[27–32] and by Kroenke and Lattimer.[33–37] Morley[9] also reported the commercial use of molybdenum and zinc compounds as smoke suppressors in PVC formulations, normally supported in inert fillers such as calcium carbonate or talc. However, the study of exfoliated/intercalated clay interactions with copper, molybdenum, and zinc oxides as potential flame retardants and smoke suppressants in PVC formulations are not known in the academic community. The objectives of this research was the study of the dehydrochlorination process, combustibility, and smoke-emission properties of nanocomposites based on PVC/organically modified montmorillonite (O-MMT) with copper, molybdenum, and zinc oxides to verify possible interactions between these factors.

EXPERIMENTAL

Materials

The formulation of the PVC compound, taken as a reference and summarized in Table I, was based in common practices used in PVC cable transformers in Brazil. PVC resin with a *K* value of 65 ± 1 (Norvic SP 1000, Braskem S/A, Camaçari, Brazil) was used as the polymer matrix. The other components of the basic formulation are detailed in Table I and were acquired from commercial sources. Table II shows the complete details of the formulations assessed in this study.

The clay used was Cloisite 30B, supplied by Southern Clay Products, Inc. (Gonzales, TX) and widely used in other studies involving PVC nanocomposites.[24,38–45] It is a natural montmorillonite, modified with a methyl-2-hydroxyethyl based quaternary ammonium salt, coupled to a fatty chain of animal origin (tallow), with approximately 65% C_{18},

TABLE I
PVC Compound Formulation Used in This Study

Component	Amount (phr)
Norvic SP 1000 (PVC resin K 65)	100
Naftomix XC-1202 (Ca/Zn thermal stabilizer)	3.5
DIDP	45
Drapex 6.8 (ESO)	5
Barralev C (precipitated calcium carbonate)	40
Stearic acid	0.2

30% C_{16}, and 5% C_{14}.[46] This clay has, as a reference, an interlayer spacing value (d_{001}) of 1.85 nm [X-ray diffraction (XRD)] and was incorporated in 2.5 and 5 wt % dosages.

Nanocomposite preparation

Where applicable, the clay was preexfoliated in a hot diisodecylphtalate (DIDP)/epoxidized soybean oil (ESO) mixture, according to the procedure described in refs. 42 and 45. In this process, the amount of plasticizer needed for each formulation was heated at 90–100°C in a beaker over a heating plate. The clay needed for the formulation was then submitted to shear, in the presence of the plasticizers, through a Fisatom (São Paulo, Brazil) 7137 (70 W) intensive mixer at 1200–1300 rpm for 20 min.

All formulations were homogenized through a Mecanoplast (Rio Claro, Brazil) ML-9 intensive mixer. Initially, the resin, thermal stabilizer, calcium carbonate, stearic acid, and, where applicable, metallic oxides were added to the mixer at room temperature, and after they were submitted to shear up to 80°C, the plasticizers DIDP and ESO were incorporated, along with the preintercalated/exfoliated clay. The final composition was discharged at 110°C; it was then cooled at 35–40°C to prevent the formation of agglomerates.

The formulations were then processed in a Miotto (São Bernardo do Campo, Brazil) LM 03/30 single-screw extruder (30 mm, length/diameter = 25) through a temperature profile of 140–145–150°C and 80 rpm. Test specimens were obtained from the pellets in a Mecanoplast laboratory two-roll mill. The temperature, processing time, and rotation to prepare 3 mm thick plates, from which the test specimens were taken, were 160°C, 3 min, and 20 rpm, respectively. The material pressing was performed in a stainless steel Luxor press (São Paulo, Brazil) at 175°C.

Morphological evaluation of the nanocomposites

The morphology of the nanocomposites was evaluated[42] with two complementary techniques:[47,48] XRD and transmission electron microscopy (TEM). X-ray diffractograms were obtained from pressed samples in a Siemens (Karlsruhe, Germany) D500 diffractometer in the reflection mode through an X-ray beam of Cu Kα (λ = 1.54 Å). Scans were performed from 2θ = 1 to 2θ = 45° with a 0.05° step. Thin samples (ca. 70 nm thick) of each formulation were obtained in a Leica (Wetzlar, Germany) EM FC6 ultramicrotome with a Drukker (Williston, VT) 3-mm/45° diamond blade at −140°C. TEM observations of these thin samples were performed in a JEOL (Tokyo, Japan) JEM-1200 EX II transmission electron microscope at 80 kV.

Combustion properties

The risk that a given material offers, when one considers fire, depends on a combination of different factors, such as[49] the ignitability, ease of extinction, flame propagation, heat release, smoke obscuration, and toxicity of the smoke released.

The combustion and smoke-release properties of the nanocomposites were assessed with different and complementary techniques. It is accepted as a current opinion[1,4,20,50–60] that the cone calorimeter technique is one of the most complete methodologies normally available to assess the combustion and smoke-release properties in a representative manner in a single, quick, and relatively simple test. Cone calorimeter measurements were made with a Stanton Redcroft FTT (Fire Test Technology, East Grinstead, UK) instrument according to the procedures described in ISO 5660-1 in specimens measuring 100 × 100 × 3 mm^3 in duplicate for each formulation under an incident heat flux of 50 kW/m^2 and a duct flow rate equal to 24 L/s. The specimens were protected by aluminum foil and propped on a ceramic support so that only the upper face was exposed to the radiant heat flux and subjected to a temperature of 20°C and a relative humidity of 30% before testing.

The ease of extinction of the nanocomposites was assessed through a limiting oxygen index (LOI) test, according to ASTM D 2863-06a with FTT equipment, with three specimens for each formulation. The tests were conducted at a temperature of 23 ± 2°C and a relative humidity of 50 ± 5%.

TABLE II
Complete Description of the PVC Formulations Evaluated in This Study

Identification	PVC base compound (%)	Metallic oxides (%)	O-MMT (%)
PVC-0-0	100	0	0
PVC-0-2.5	97.5	0	2.5
PVC-0-5	95	0	5
PVC-5-0	95	5	0
PVC-5-2.5	92.5	5	2.5
PVC-5-5	90	5	5
PVC-10-0	90	10	0
PVC-10-2.5	87.5	10	2.5
PVC-10-5	85	10	5

Thermogravimetry (TG) coupled to mass spectroscopy (MS)

One of the objectives of this study was to assess the effects of metallic oxides and O-MMT on the dehydrochlorination and smoke-release behavior of the PVC nanocomposites and to correlate the chemical species released during the pyrolysis process and the effects observed in the cone calorimeter test. The different formulations were assessed as to stability to heat with a STA 409 thermobalance coupled to a QMS 403 mass spectrometer, both from Netzsch Analyzing and Testing (Selb, Germany), with alumina crucibles in a synthetic air atmosphere with a gas flow of 50 mL/min. Scans were conducted between room temperature and 1000°C at a heating rate of 20°C/min.

Scanning electronic microscopy (SEM)

SEM observations were made with a Philips XL 30 instrument (FEI Company, Hillsboro, OR), operated at 20 kV, equipped with an Edax energy-dispersive X-ray spectroscope (model New XL 30). Analyzed samples were obtained from the nanocomposite pyrolysis in a CEM Phoenix Airwave microwave muffle furnace (Matthews, NC) at 600°C for 1 h. The ashes resulting from this process were covered with a thin gold film with a Bal-Tec SCD 005 sputter (Leica Microsystems, Wetzlar, Germany), operated at 60 mA and 10^{-1} mbar for 100 s. Some selected samples were automatically covered with a thin carbon film to allow the analysis of molybdenum through energy-dispersive X-ray spectroscopy (EDS). Unfortunately, this metal's main peaks overlapped gold's peaks in the resulting spectrum, which made identification impossible.

Statistical analysis

Statistical analyses were performed via Microsoft Excel. More sophisticated analyses, such as the evaluation of the effects of the different variables studied in this experimental project (content of metallic oxides and O-MMT), were carried out with Minitab 15 (Minitab, Inc., Sate College, PA) and Design-Expert 7.1 (StatEase, Inc., Minneapolis, MN), as the formulations evaluated corresponded to a factorial design of experiments with two factors at three levels.

RESULTS AND DISCUSSION

Morphological evaluation of the nanocomposites

In a previous article,[45] we presented X-ray diffractograms and TEM observations made with the different nanocomposites prepared in this study. With both techniques, it was possible to attest the formation of the PVC/O-MMT nanocomposites with a hybrid intercalated/partially exfoliated structure. We also presented a more detailed assessment of the nanocomposite formation.

Combustion properties

Table III gives a summary of the main results taken in the cone calorimeter and in the LOI tests, presented according to the metallic oxides content in the nanocomposite. A summary of design of experiment (DOE) analysis results is also shown, including the p results for the effects of the metallic oxides and O-MMT contents incorporated to the nanocomposites, as well as their interactions, analyzed with Design-Expert 7.1.

Figure 1 shows the heat-release curves as a function of time for the nanocomposites, grouped according to the metallic oxides content in the formulations. Observing the curves in Figure 1 and the data in Table III for the peak heat-release rate (PHRR), we concluded that neither the metallic oxides content nor the O-MMT content present in the nanocomposite formulations had a statistically significant effect on this parameter. However, for the values of the mean heat-release rate (MHRR) and the total heat released (THR; corresponding to the integration of the curves), the effects of metallic oxides content in the nanocomposite formulations were statistically significant, which was denoted by $p < 0.0001$. The presence of metallic oxides significantly affected the samples' heat-release profile because growing quantities of metallic oxides shifted the peaks of heat-release rate (HRR) to longer time periods and reduced the areas under the curves, which is important from a material safety perspective in fire situations.[1,2,6–8] On the other hand, the effects of O-MMT content were not statistically significant for altering the MHRR and THR values. In other words, the presence of clay, even when it was intercalated/partially exfoliated, apparently did not alter significantly the heat-release properties during the combustion of the nanocomposites studied herein. The same was observed for the effects of both factors in the average specific mass loss rate (ASMLR) of the specimens: apparently, O-MMT, even when it was intercalated/partially exfoliated, did not significantly affect the nanocomposite pyrolysis rate. In other words, at least in this case, the barrier effect was negligible. Figure 2 shows the results of the time-dependent mass loss rate (MLR), showing a strong correlation with the samples' HRR. Here, once again, the effects of the presence of metallic oxides were significant from a statistical perspective ($p = 0.0003$), whereas the effects of O-MMT were again negligible. However, the software used for DOE analysis revealed that the presence of O-MMT caused some sort of interaction with the metallic oxides, at least in the MHRR, THR, mean effective heat of combustion (MEHC), and ASMLR variables.

TABLE III
Cone Calorimetry (50 kW/m^2) and LOI Results for the PVC/Metallic Oxides/O-MMT Nanocomposites

Formulation	O-MMT (wt %)	PHRR (kW/m^2)	MHRR (kW/m^2)	THR (MJ/m^2)	MEHC (MJ/kg)	ASMLR (g s^{-1} m^{-2})	TSP (m^2/kg)	MCO (kg/kg)	CR (%)	NCR (%)	LOI (%)
					$CuO/MoO_3/ZnO = 0$ wt %						
PVC-0-0	0.0	285 ± 11	130 ± 5	66.1 ± 0.1	18.5 ± 0.1	11.8 ± 2.3	736 ± 21	0.054 ± 0.004	26.0 ± 0.1	26.0 ± 0.1	23.0
PVC-0-2.5	2.5	243 ± 3	127 ± 18	59.6 ± 15.2	16.6 ± 3.5	13.0 ± 1.8	617 ± 29	0.063 ± 0.002	27.5 ± 0.5	26.8 ± 0.5	23.4
PVC-0-5	5.0	276 ± 58	139 ± 21	61.6 ± 0.3	17.4 ± 2.3	14.2 ± 1.7	622 ± 27	0.065 ± 0.006	28.0 ± 1.0	26.6 ± 0.9	24.0
					$CuO/MoO_3/ZnO = 5$ wt %						
PVC-5-0	0.0	191 ± 15	100 ± 3	44.6 ± 1.6	14.1 ± 0.1	12.0 ± 0.8	387 ± 13	0.060 ± 0.000	37.3 ± 0.5	35.4 ± 0.5	26.4
PVC-5-2.5	2.5	202 ± 17	99 ± 8	44.3 ± 6.2	14.5 ± 0.2	11.5 ± 2.0	373 ± 26	0.066 ± 0.003	38.0 ± 0.3	34.2 ± 0.3	25.6
PVC-5-5	5.0	224 ± 8	110 ± 4	45.9 ± 2.1	15.0 ± 0.1	12.0 ± 0.2	369 ± 37	0.064 ± 0.001	39.4 ± 0.5	35.4 ± 0.5	25.0
					$CuO/MoO_3/ZnO = 10$ wt %						
PVC-10-0	0.0	233 ± 26	97 ± 1	44.4 ± 2.2	13.7 ± 0.5	11.8 ± 1.2	388 ± 17	0.066 ± 0.002	40.2 ± 0.2	36.1 ± 0.1	28.0
PVC-10-2.5	2.5	209 ± 3	94 ± 1	45.5 ± 0.4	14.5 ± 0.2	10.7 ± 0.3	339 ± 21	0.074 ± 0.001	41.7 ± 0.1	36.5 ± 0.1	26.4
PVC-10-5	5.0	274 ± 8	90 ± 12	47.5 ± 3.7	15.1 ± 0.2	9.6 ± 1.1	314 ± 4	0.074 ± 0.001	42.6 ± 0.8	36.2 ± 0.7	26.2
					DOE Summary (Design-Expert 7.1-: Effects (p values)						
Parameter	PHRR (kW/m^2)	MHRR (kW/m^2)	THR (MJ/m^2)	MEHC (MJ/kg)	ASMLR (g s^{-1} m^{-2})	TSP (m^2/kg)	MCO (kg/kg)	CR (%)	NCR (%)	LOI (%)	
Intercept		273	128	65.0	18.1	11.8	711	0.055	26.1	35.0	23.3
		(0.0025)	(<0.0001)	(<0.0001)	(0.0012)	(0.0003)	(<0.0001)	(<0.0001)	(<0.0001)	(<0.0001)	(0.0014)
Metallic oxides		−22	−7	−5.7	−1.0	0.0 (0.0004)	−84	0.000	+ 3.0	+ 4.9	+ 0.5
		(0.1107)	(<0.0001)	(<0.0001)	(0.0001)	(0.0004)	(<0.0001)	(<0.0001)	(<0.0001)	(<0.0001)	(0.0004)
O-MMT		−32	−1	−2.3	−0.5	+ 0.5	−39	+ 0.005	+ 0.6	+ 0.1	+ 0.1
		(0.1426)	(0.3937)	(0.9987)	(0.5081)	(0.9947)	(0.0009)	(<0.0001)	(<0.0001)	(0.4544)	(0.1229)
Interaction	No	Yes	Yes	Yes	Yes	No	No	No	No	No	

Cone calorimeter parameters: PHRR = peak heat release rate; MHRR = mean heat release rate; THR = total heat released; MEHC = mean effective heat of combustion; ASMLR = average specific mass loss rate; TSP = total smoke production; MCO = mean CO; CR = char residue; NCR = normalized char residue. For a detailed description of these parameters, please see ref. 52.

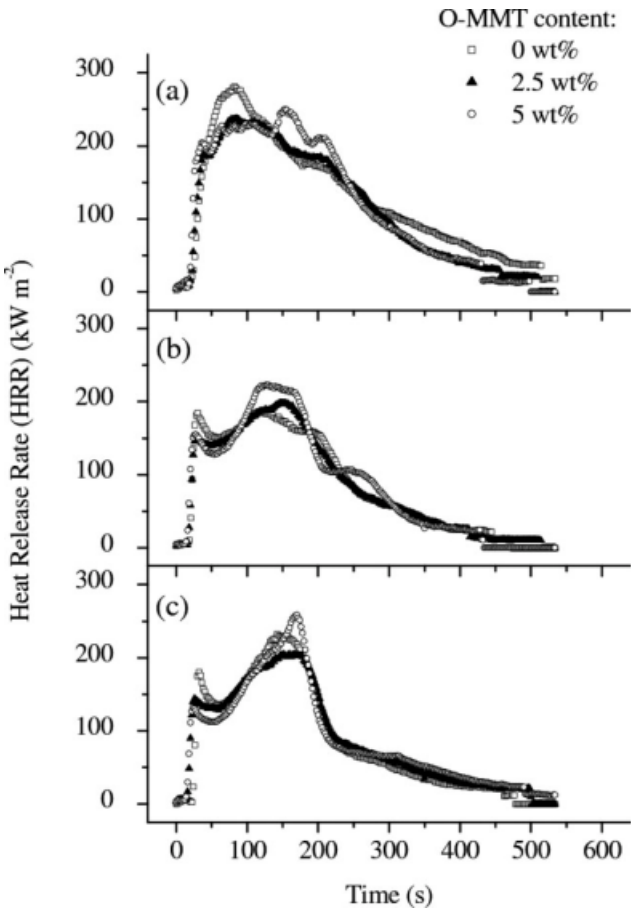

Figure 1 HRR curves for the PVC/metallic oxides/O-MMT nanocomposites as a function of the metallic oxides content: (a) 0, (b) 5, and (c) 10 wt %.

MEHC values were affected according to the statistical data by the metallic oxides content ($p = 0.0012$). Because the MEHC value was determined in the cone calorimeter from gas-phase data,[50] we concluded that the metallic oxides somehow affected the composition of gases that fed the combustion zone, making them energetically less rich and reducing the MHRR and THR values, as mentioned before. Figure 3 shows the CO production rate curves versus time for the nanocomposites, grouped according to the metallic oxides content in the formulations. The metallic oxides altered the CO production rate in a statistically significant manner ($p < 0.0001$), like the O-MMT content found in the nanocomposites. This change in CO production behavior, plus the reduction in MEHC, provided strong evidence of a change in the samples' combustion mechanism, which was a clear function of the compositional factors and suggested that a less rich fuel and an incomplete combustion mechanism were introduced in the system.[56,57] The MEHC results obtained herein, despite the statistical consistency, were the opposite of those obtained by Li and Wang[52,54,58–60] in studies with copper and molybdenum oxides incorporated into rigid PVC compounds. According to these authors, volatile substances of easier combustion were formed as a result of the presence of metallic oxides, which explained the increase in the MEHC values they found. However, the same cone calorimeter runs exhibited an increase in the CO production rate, but the authors did not comment about this observation.

Figure 4 show the rate of smoke release curves as a function of time for the nanocomposites, grouped according to the metallic oxide content in the formulations. It was possible to verify that both factors had a statistically significant effect on smoke. As shown in Figure 4, the presence of metallic oxides in the PVC formulations reduced the rate of smoke released and also promoted a delay in reaching the peak; this is, once again, favorable for material safety in fire situations.[1,2,6–8] The O-MMT effects were somewhat statistically significant, as shown in Table III ($p = 0.0009$), for total smoke produced (TSP); however, it was clear that the effects of the metallic oxide amount was more significant than the effects caused by the amount of O-MMT. In this case, it

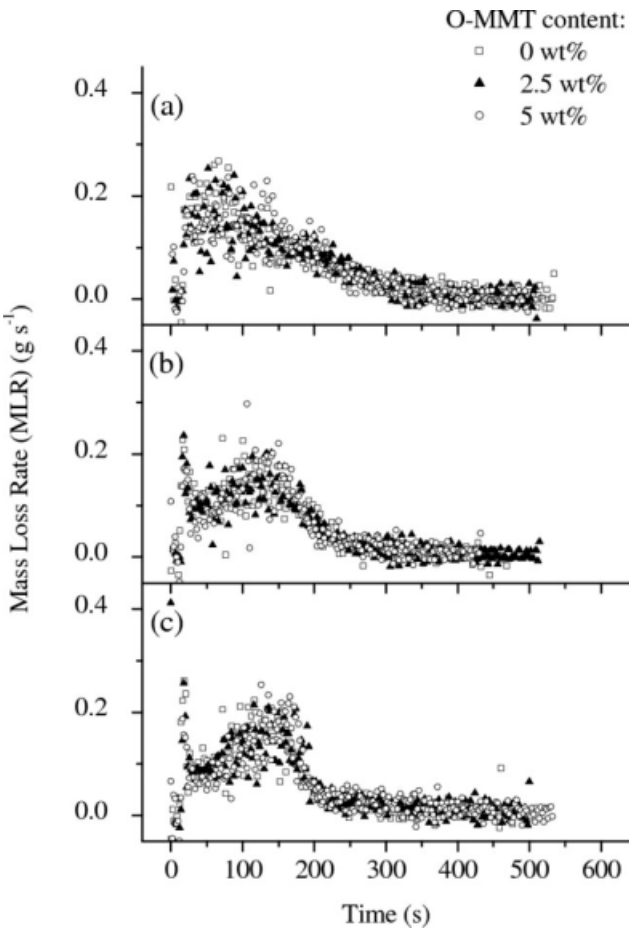

Figure 2 MLR curves for the PVC/metallic oxides/O-MMT nanocomposites as a function of the metallic oxides content: (a) 0, (b) 5, and (c) 10 wt %.

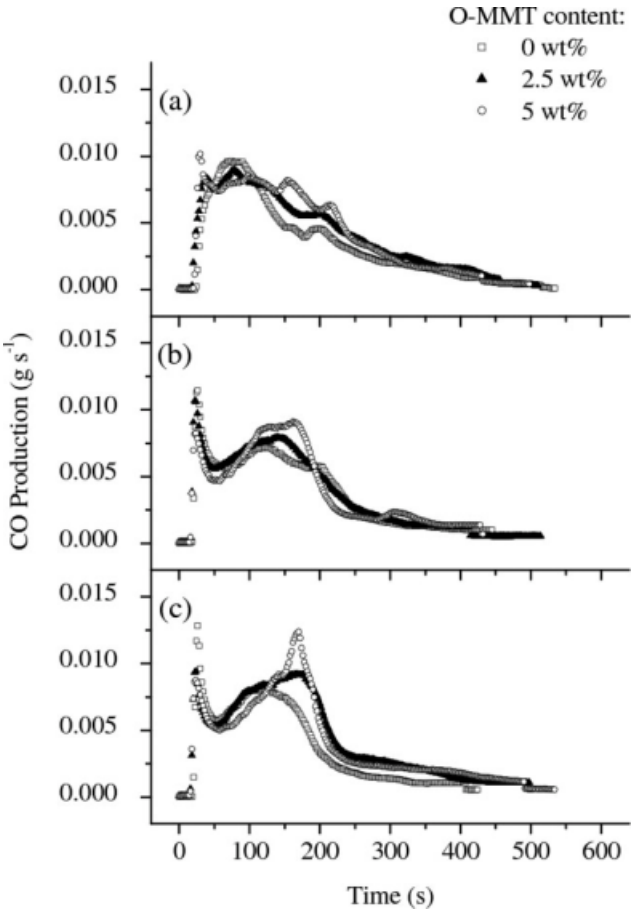

Figure 3 Carbon monoxide production curves for the PVC/metallic oxides/O-MMT nanocomposites as a function of the metallic oxides content: (a) 0, (b) 5, and (c) 10 wt %.

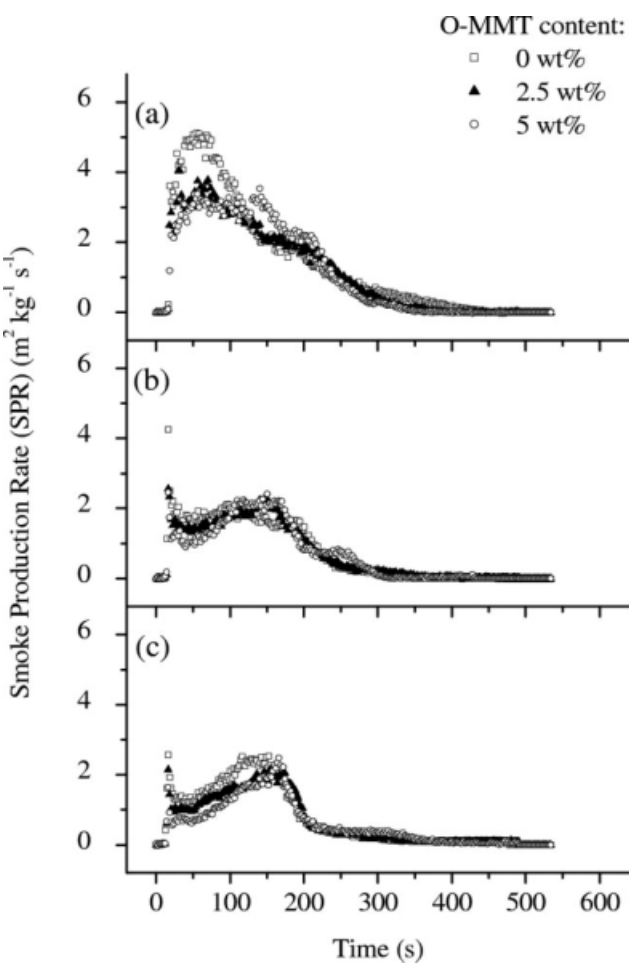

Figure 4 Smoke production rate curves for the PVC/metallic oxides/O-MMT nanocomposite, as a function of the metallic oxides content: (a) 0, (b) 5, and (c) 10 wt %.

was not possible to observe any interaction between the two factors studied.

The quantity of char residue (CR) remaining from the specimen at the end of the cone calorimeter test is another important parameter related to the smoke released by materials during combustion, simply because one of the main mechanisms for reducing smoke is the fixation of organic matter in the solid phase, which retards/prevents its pyrolysis and consequent combustion.[1,4,27–37] As verified in Table III, both factors studied had statistical significance in relation to the CR values. However, it is important to remember that the nanocomposite formulations had an important amount of inorganic material incorporated into them. Thus, it was to be expected that formulations with greater amounts of inorganic additives resulted in greater residue values at the end of combustion, which could not be carbonaceous char. To normalize the values for the diverse formulations studied herein, an additional column is shown in Table III that corresponds to the normalized char residue (NCR) value for each formulation. We determined the NCR values by multiplying the CR value measured in the cone calorimeter test for each formulation by the mass fraction of the PVC base compound, as shown previously in Table II. Thus, all of the formulations were compared, with

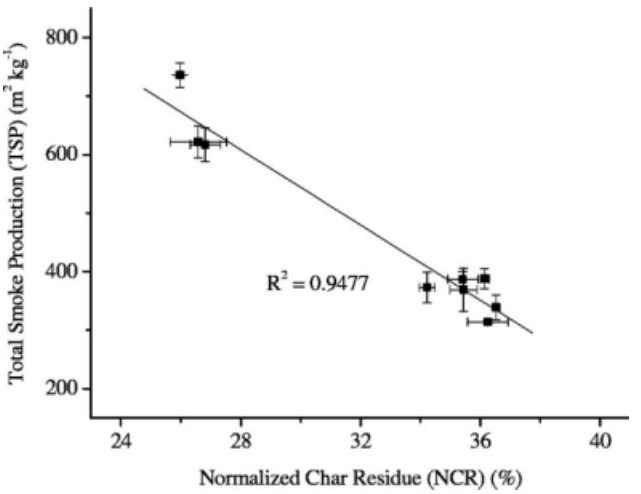

Figure 5 Correlation between TSP and NCR.

TABLE IV
TG/MS Results for the PVC/Metallic Oxides/O-MMT Nanocomposites

Formulation	O-MMT (wt %)	T_{ONSET} (°C)	T_{PDR} (°C)	R_{PDR} (%/min)	Char yield (%)	$Area_{HCl}$ ($\times 10^{-10}$ A min/mg)	T_{HCl} (°C)	$Area_{C6H6}$ ($\times 10^{-12}$ A min/mg)	T_{C6H6} (°C)
				$CuO/MoO_3/ZnO = 0$ wt %					
PVC-0-0	0.0	233.6	331.5	22.1	18.1	8.36	331.5	47.5	317.4
PVC-0-2.5	2.5	240.2	321.0	23.2	17.4	5.01	325.8	24.2	305.4
PVC-0-5	5.0	222.7	309.8	19.1	17.7	5.34	319.2	21.6	305.2
				CuO/MoO3/ZnO = 5 wt %					
PVC-5-0	0.0	235.8	258.0	42.1	16.8	6.55	256.5	10.9	258.0
PVC-5-2.5	2.5	229.3	256.6	38.7	21.7	3.75	361.3	9.59	247.2
PVC-5-5	5.0	227.1	252.8	32.6	20.4	3.07	251.5	7.54	239.0
				$CuO/MoO_3/ZnO = 10$ wt %					
PVC-10-0	0.0	229.3	252.3	41.4	9.1	3.58	253.9	11.5	239.8
PVC-10-2.5	2.5	224.9	253.4	27.8	21.3	3.11	255.2	8.82	242.7
PVC-10-5	5.0	222.7	240.5	29.5	19.6	3.45	271.6	8.24	251.2
				DOE summary (Design-Expert 7.1): Effects (p values)					
Parameter	T_{ONSET} (°C)	T_{PDR} (°C)	R_{PDR} (%/min)	Char yield (%)	$Area_{HCl}$ ($\times 10^{-10}$ A min/mg)	T_{HCl} (°C)	$Area_{C6H6}$ ($\times 10^{-12}$ A min/mg)	T_{C6H6} (°C)	
Intercept		237.1	328.7	23.7	17.1	7.22	324.4	43.4	319.6
		(0.0574)	(0.0017)	(0.0632)	(0.2003)	(0.0164)	(0.1712)	(0.0521)	(0.0060)
Metallic oxides		−0.7	−19.3	+ 5.8	+ 0.3	−0.29	−6.5	−7.68	−19.2
		(0.1135)	(0.0003)	(0.0344)	(0.6413)	(0.0160)	(0.0709)	(0.0162)	(0.0011)
O-MMT		−1.7	−1.3	−1.7	+ 2.4	−0.44	0.0	−7.37	−6.3
		(0.0481)	(0.0401)	(0.0784)	(0.1141)	(0.0424)	(0.9966)	(0.0906)	(0.2955)
Interaction		No	No	No	Yes	No	No	No	Yes

TG/MS parameters: T_{ONSET} = temperature of the onset of dehydrochlorination (TG); T_{PDR} = temperature at the peak decomposition rate (dTG); R_{PDR} = rate of mass loss at the peak decomposition rate (dTG); $Area_{HCl}$ = integration result of the QMID HCl versus temperature curve; T_{HCl} = peak temperature of the QMID HCl versus temperature curve; $Area_{C6H6}$ = integration result of the QMID C_6H_6 versus temperature curve; T_{C6H6} = peak temperature of the QMID C_6H_6 versus temperature curve.

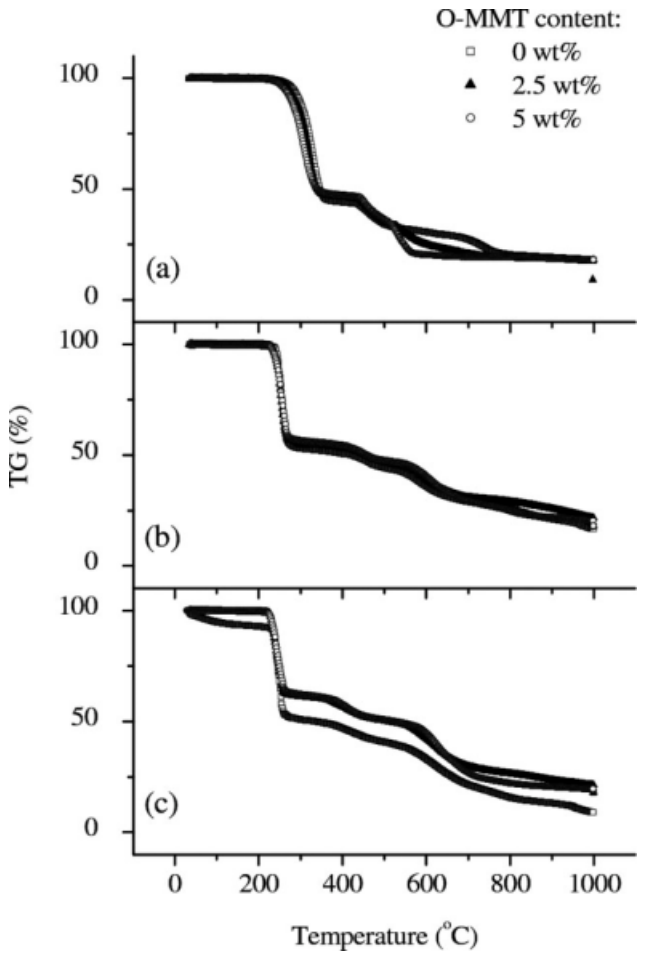

Figure 6 TG curves for the PVC/metallic oxides/O-MMT nanocomposites as a function of the metallic oxides content: (a) 0, (b) 5, and (c) 10 wt %.

the PVC formulation taken as a reference. However, an analysis of the NCR results demonstrated that only the effect of the metallic oxides content was statistically significant, and that the effect of O-MMT content was negligible; this agreed with what was observed for MLR. These results corroborated several studies conducted by Starnes and coworkers,[27–32] Kroenke and Lattimer,[33–37] and Li and Wang[19,52–54,58–60] and confirmed that the mechanism of action of the main smoke suppressants used in PVC involves Diels–Alder condensation reactions and the formation of benzene and other aromatic compounds. According to these authors, additives based on molybdenum interfere in the dehydrochlorination process and in the formation of polyenic sequences in PVC. They anticipate this process and force the formation of a carbonaceous char and also induce the formation of *trans*-polyenes structures instead of *cis*-polyenes. Thus, the formation of benzene and other aromatic structures is reduced by the impossibility of carbon–carbon bond rotations, so the preferential termination mode for the dehydrochlorination reaction becomes the Diels–Alder condensation and promotes the fixation of more carbon and hydrogen in the CR and a more reduced tendency for soot and smoke formation. Likewise, additives based on copper and zinc accelerate dehydrochlorination reactions and increase their rate. Copper, in particular, acts as an inductor agent in Diels–Alder condensation reactions through a reductive coupling mechanism; this further favors the fixation of carbon and hydrogen in the form of carbonaceous residue and acts in synergy with molybdenum compounds. Figure 5 shows that there is a high correlation between TSP and NCR values for the studied formulations.

Finally, the LOI results show that the effects of the metallic oxides content were statistically significant. In other words, the greater the content of these additives in the nanocomposite formulations was, the greater the difficulty to sustain the combustion was, as denoted by the increase in the LOI values. The effect of O-MMT content again proved to be negligible.

TG/MS

Table IV shows a summary of the main TG/MS results, presented according to the metallic oxides

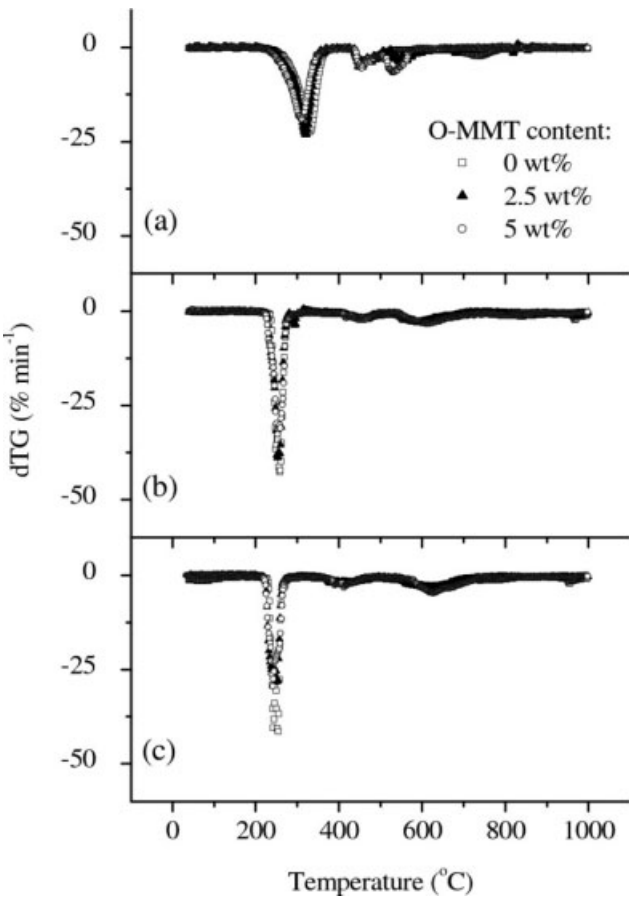

Figure 7 dTG curves for the PVC/metallic oxides/O-MMT nanocomposites as a function of the metallic oxides content: (a) 0, (b) 5, and (c) 10 wt %.

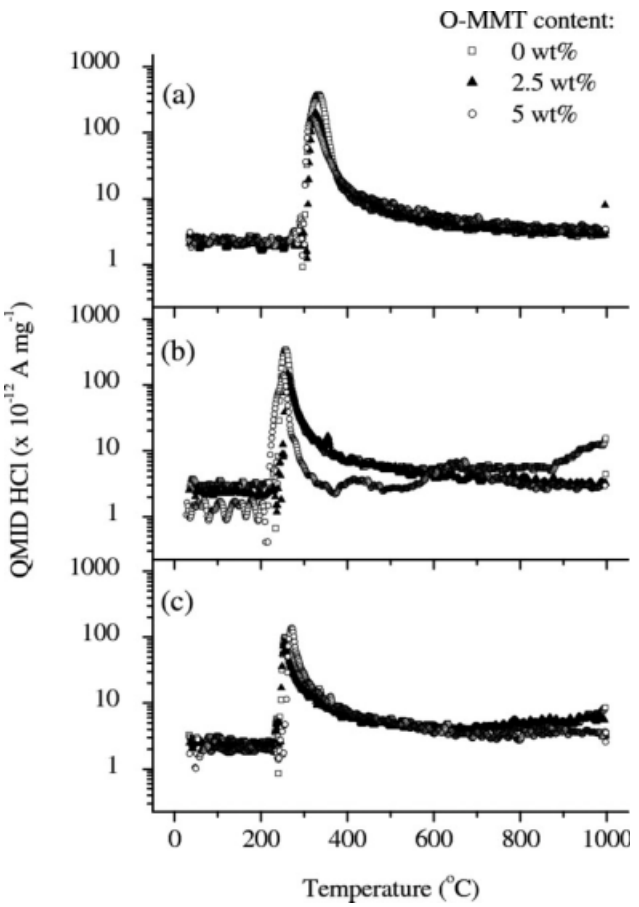

Figure 8 MS curves for HCl released during the pyrolysis of the PVC/metallic oxides/O-MMT nanocomposites as a function of the metallic oxides content: (a) 0, (b) 5, and (c) 10 wt %.

content in the nanocomposites. A summary of the DOE analysis results is also shown, including p results for the effects of metallic oxides and O-MMT contents incorporated into the nanocomposites, and their interactions, analyzed with Design-Expert 7.1.

Figures 6 and 7 show the thermogravimetry (TG; Fig. 6) and the derivative thermogravimetry (dTG; Fig. 7) curves for the nanocomposites, grouped according to the metallic oxides content in the formulations. In both curves and in the data shown in Table IV, we observed that the presence of metallic oxides accelerated the dehydrochlorination process and promoted peaks at lower temperatures and intensified peak MLRs. The presence of metallic oxides and O-MMT were statistically significant ($p \leq 0.05$) in relation to the onset temperature (T_{ONSET}) and peak temperature of the decomposition rate (T_{PDR}); however, only metallic oxides content had a statistically significant effect on the rate of mass loss at the peak decomposition rate (R_{PDR}). These results corroborated the cone calorimeter observations presented before and the diverse studies carried by Starnes and coworkers,[27–32] Kroenke and Lattimer,[33–37] and Li and Wang.[19,52–54,58–60]

The use of the TG/MS coupling technique revealed important data about the sample degradation mechanisms. Figures 8 and 9 show the mass spectroscopy detection rate (QMID) curves for HCl (Fig. 8) and benzene (Fig. 9) for the nanocomposites, grouped according to the metallic oxides content in the formulations. As observed for TG, an acceleration in the dehydrochlorination process was verified because the peaks of HCl release rate occurred at lower temperatures, with virtually the same intensities among the different formulations. A strong and significant reduction in the formation of benzene was observed qualitatively, as shown in Figure 9, and quantitatively from the integration data of the QMID versus time curves, as shown in Table IV, because of the presence of metallic oxides in the formulations ($p = 0.0162$), which once again confirmed and demonstrated the mechanisms proposed by Starnes and coworkers,[27–32] Kroenke and Lattimer,[33–37] and Li and Wang.[19,52–54,58–60]

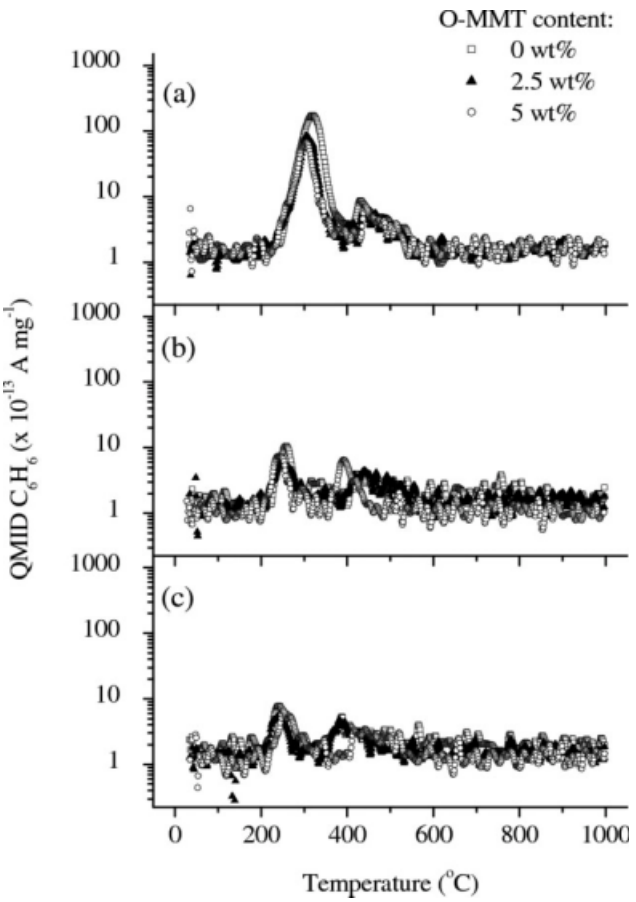

Figure 9 MS curves for benzene released during the pyrolysis of the PVC/metallic oxides/O-MMT nanocomposites as a function of the metallic oxides content: (a) 0, (b) 5, and (c) 10 wt %.

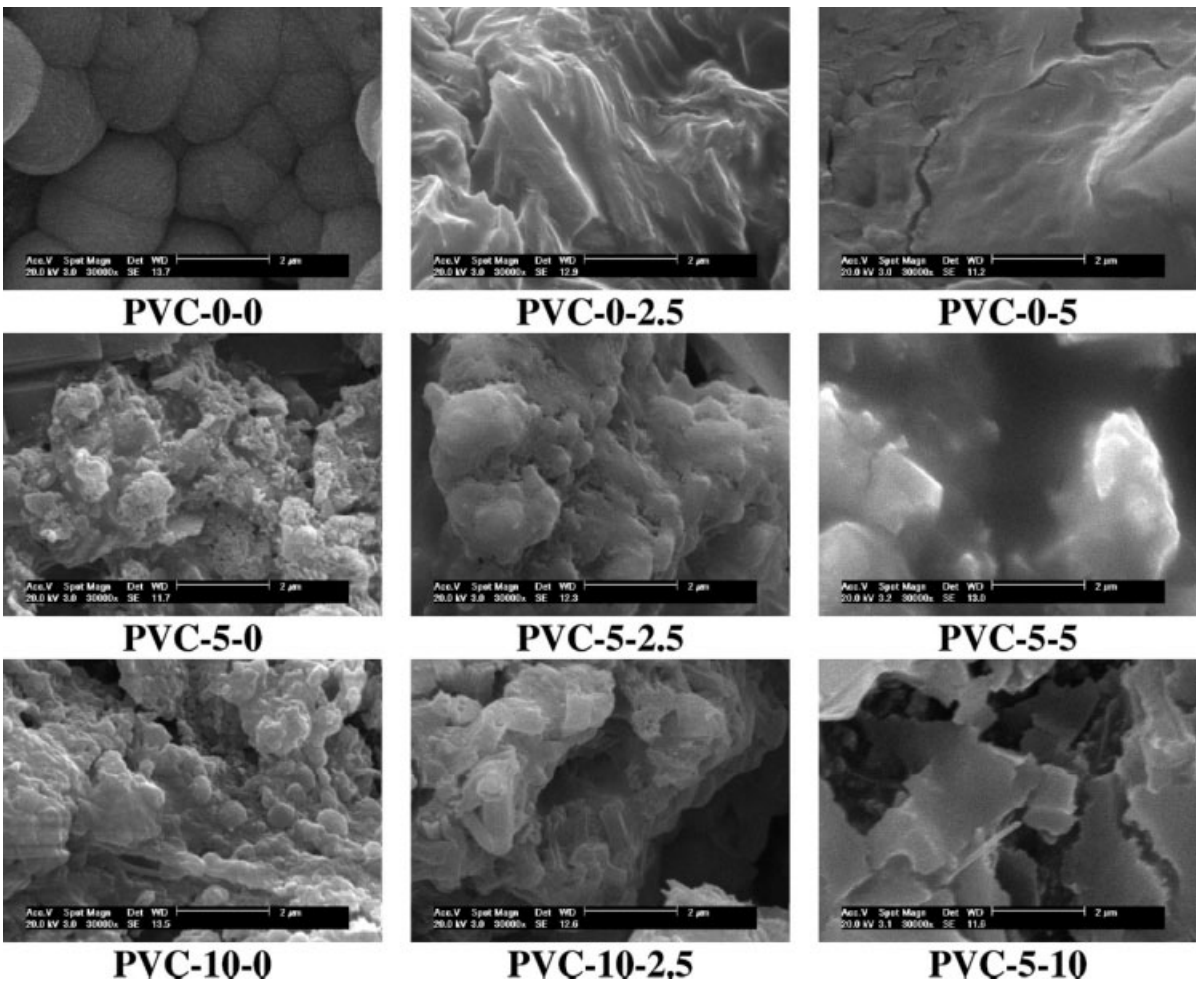

Figure 10 SEM images for the PVC/metallic oxides/O-MMT nanocomposites.

SEM

Figures 10 and 11 show SEM observations (Fig. 10) and EDS results (Fig. 11) for the ashes resulting from the pyrolysis of nanocomposites, grouped according to the metallic oxide content in the formulations. Figure 10 shows different morphologies for the carbonaceous char as a result of the composition of the formulation. Specifically, in those cases where O-MMT was present, some tactoids were seen. Because these samples were coated with gold during preparation, the qualitative assessment of atomic species present through EDS, especially for molybdenum, was compromised. For this reason, some samples (PVC-0-0, PVC-5-0, and PVC-5-5) were selected and reprepared; this time, they were coated with carbon rather than gold. This allowed for better definition of the peaks of the atomic species with EDS. This technique, used to detect traces of elements, as shown in Figure 11, was effective at detecting copper and molybdenum in the ashes resulting from the combustion process of the nanocomposites. However, zinc was not observed in the PVC-5-0 (5 wt % metallic oxides) ashes or in the PVC-5-5 (5 wt % metallic oxides + 5 wt % O-MMT) ashes, which suggest that its effect, at least at the end of combustion process, occurred in the gas phase. Another hypothesis is that zinc sublimated during the pyrolysis cycle in the muffle furnace because its vaporization temperature (907°C at 760 mmHg) was significantly lower than copper (2762°C at 760 mmHg) and molybdenum (5569°C at 760 mmHg).[61] New studies of the composition and reaction kinetics in the gas phase need to be conducted in the future to confirm these hypotheses.

CONCLUSIONS

Nanocomposites of PVC, metallic oxides, and O-MMT were prepared in a melt-blending or intercalation-in-the-molten-state process. The formation of an intercalated/partially exfoliated hybrid microstructure was confirmed by XRD measurements and

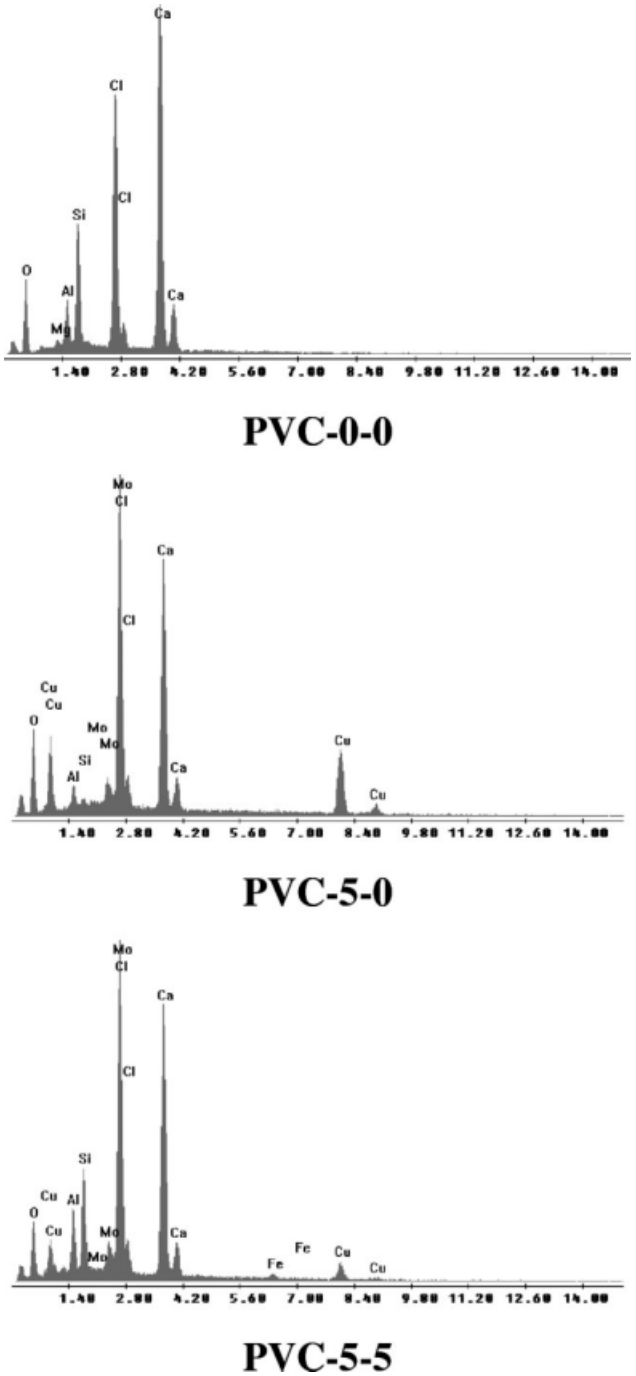

Figure 11 EDS traces for selected PVC/metallic oxides/O-MMT nanocomposites.

TEM observations in every situation studied. The combustion and smoke-release properties, when studied with cone calorimetry in a radiant heat flux of 50 kW/m^2, revealed that the metallic oxides had a very significant effect on the combustion and smoke-suppression properties, especially those most important regarding safety requirements in fire situations, retarding heat, and smoke release, and reduced their absolute quantities. The presence of O-MMT only discretely affected these properties, and little interaction was observed in the joint use of these two additives.

The cone calorimeter measurements offered strong indications that metallic oxides significantly affected the combustion mechanisms of the nanocomposites studied herein. They affected both the mean heat of combustion (MEHC) and the carbon monoxide released values; this indicated the occurrence of a less efficient combustion process, possibly resulting from the generation of a less rich fuel and/or incomplete combustion mechanisms introduced in the system. This study did not reveal whether these effects resulted from mechanisms introduced in the solid phase and/or the gaseous phase; however, the absence of zinc in ashes, when studied by SEM/EDS, indicated the need for a more in-depth analysis of this topic in the future.

The results also confirm the mechanisms proposed by Starnes and coworkers,[27–32] Kroenke and Lattimer,[33–37] and Li and Wang,[19,52–54,58–60] that is, the anticipation of dehydrochlorination, reductive coupling, and benzene suppression, which resulted from the presence of the copper, molybdenum, and zinc metals. These phenomena were observed in the TG/dTG results, the increase in postcombustion carbonaceous CR in the cone calorimeter, and in the significant reduction in benzene formation during combustion, in the latter case, as indicated in the TG/MS measurements obtained.

The authors are grateful for the support given by Braskem S/A, through the Núcleo de Estudos Orientados do PVC (NEO PVC) program, and for the contributions from Rafael Laurini, Lucas Polito, Max Sakuma, Carlos Calmanovici, Mauro Oviedo, and Cristóvão de Lemos, from Braskem S/A; Eduardo Perosa, Maurício França, and Miriam Vianna from Centro de Microscopia e Microanálises da Pontifícia Universidade Católica do Rio Grande do Sul (CEMM/PUCRS) and João Mesquita and Richard Lopes from Netzsch do Brasil Indústria e Comércio, Ltd., which were fundamental for the completion of this work.

References

1. Innes, J.; Innes, A. Plastic Flame Retardants: Technology and Current Developments; Rapra Technology: Shropshire, England, 2003.
2. Bourbigot, S.; Le Bras, M.; Troitzsch, J. In Plastics Flammability Handbook: Principles, Regulations, Testing, and Approval, 3rd ed.; Troitzsch, J., Ed.; Hanser: Munich, 2004; Chapter 1.
3. Quinalia, E. Construção Mercado 2007, 72, 60.
4. Hirschler, M. M. In PVC Handbook; Wilkes, C. E.; Summers, J. W.; Daniels, C. A., Eds.; Hanser Gardner: Cincinnati, OH, 2005.
5. Le Bras, M.; Price, D.; Bourbigot, S. In Plastics Flammability Handbook: Principles, Regulations, Testing, and Approval, 3rd ed.; Troitzsch, J., Ed.; Hanser: Munich, 2004; Chapter 7.
6. Hull, T. R.; Stec, A. A.; Lebek, K.; Price, D. Polym Degrad Stab 2007, 92, 2239.
7. Norsk Hydro. PVC and the Environment 96; Norsk Hydro A. S.: Oslo, Norway, 1995.

8. British Plastics Federation. PVC in Fires. British Plastics Federation: London, 1996.
9. Morley, J. C. In Handbook of Polyvinyl Chloride Formulating; Wickson, E. J., Ed.; Wiley-Interscience: New York, 1993; Chapter 21.
10. Yang, F.; Ou, Y.; Yu, Z. J Appl Polym Sci 1998, 69, 355.
11. Lan, T.; Kaviratna, P. D.; Pinnavaia, T. J. Chem Mater 1994, 6, 573.
12. Wang, Z.; Lan, T.; Pinnavaia, T. J. Chem Mater 1996, 8, 2200.
13. Giannelis, E. P. Mater Design 1992, 13, 100.
14. Alexandre, M.; Dubois, P. Mater Sci Eng R 2000, 28, 1.
15. Utracki, L. A. Clay-Containing Polymeric Nanocomposites; Rapra Technology: Shropshire, England, 2004; Vol. 1.
16. Hull, T. R.; Lebek, K.; Pezzani, M.; Messa, S. Fire Safety J 2008, 43, 140.
17. Ramasubramanian, H. Plast Eng 2007, 63, 50.
18. Beyer, G. Plast Addit Compound 2002, 4, 22.
19. Yang, Z.; Li, B.; Tang, F. J Vinyl Addit Techn 2007, 13, 31.
20. Beyer, G. J Fire Sci 2007, 25, 65.
21. Kalendova, A.; Kovarova, L.; Malac, Z.; Malac, J.; Vaculik, J.; Hrncirik, J.; Simonik, J. Presented at Annual Technical Conference, May 5-9, 2002, San Francisco, 2002.
22. Awad, W. H.; Beyer, G.; Benderly, D.; Ijdo, W. L.; Songtipya, P.; Jimenez-Gasco, M. M.; Manias, E.; Wilkie, C. A. Polymer 2009, 50, 1857.
23. Pagacz, J.; Pielichowski, K. J Vinyl Addit Techn 2009, 15, 61.
24. Matuana, L. M. J Vinyl Addit Techn 2009, 15, 77.
25. Zestos, A. G.; Grinnell, C. L.; Vinh, L. J.; Pike, R. D.; Starnes, W. H., Jr. J Vinyl Addit Techn 2009, 15, 87.
26. Moghri, M.; Akbarian, M. J Vinyl Addit Techn 2009, 15, 92.
27. Starnes, W. H., Jr.; Edelson, D. Macromolecules 1979, 12, 797.
28. Edelson, D.; Kuck, V. J.; Lum, R. M.; Scalco, E.; Starnes, W. H., Jr. Combust Flame 1980, 38, 271.
29. Wescott, L. D., Jr.; Starnes, W. H., Jr.; Mujsce, A. M. J Anal Appl Pyrol 1985, 8, 163.
30. Pike, R. D.; Starnes, W. H., Jr.; Jeng, J. P.; Bryant, W. S.; Kourtesis, P.; Adams, C. W.; Bunge, S. D.; Kang, Y. M.; Kim, A. S.; Kim, J. H.; Macko, J. A.; O'Brien, C. P. Macromolecules 1997, 30, 6957.
31. Starnes, W. H., Jr. Prog Polym Sci 2002, 27, 2133.
32. Starnes, W. H., Jr.; Pike, R. D.; Cole, J. R.; Doyal, A. S.; Kimlin, E. J.; Lee, J. T.; Murray, P. J.; Quinlan, R. A.; Zhang, J. Polym Degrad Stab 2003, 82, 15.
33. Kroenke, W. J. J Appl Polym Sci 1981, 26, 1167.
34. Lattimer, R. P.; Kroenke, W. J. J Appl Polym Sci 1981, 26, 1191.
35. Lattimer, R. P.; Kroenke, W. J. J Appl Polym Sci 1982, 27, 1355.
36. Lattimer, R. P.; Kroenke, W. J.; Getts, R. G. J Appl Polym Sci 1984, 29, 3783.
37. Kroenke, W. J.; Lattimer, R. P. J Appl Polym Sci 1986, 32, 3737.
38. Wang, D.; Parlow, D.; Yao, Q.; Wilkie, C. A. J Vinyl Addit Techn 2001, 7, 203.
39. Yalcin, B.; Cakmak, M. Polymer 2004, 45, 6623.
40. Kovarova, L.; Kalendova, A.; Gerard, J.-F.; Malac, J.; Simonik, J.; Weiss, Z. Macromol Symp 2005, 221, 105.
41. Benderly, D.; Osorio, F.; Ijdo, W. L. J Vinyl Addit Techn 2008, 14, 155.
42. Rodolfo, A., Jr.; Mei, L. H. I. Polímeros 2009, 19, 1.
43. Peprnicek, T.; Duchet, J.; Kovarova, L.; Malac, J.; Gerard, J.-F.; Simonik, J. Polym Degrad Stab 2006, 91, 1855.
44. Peprnicek, T.; Kalendova, A.; Pavlova, E.; Simonik, J.; Duchet, J.; Gerard, J.-F. Polym Degrad Stab 2006, 91, 3322.
45. Rodolfo, A., Jr.; Innocentini-Mei, L. H., to appear.
46. Southern Clay Products. Cloisite 30B—Typical Physical Properties Bulletin. http://www.scprod.com. (accessed July 4, 2009).
47. Paul, D. R.; Robeson, L. M. Polymer 2008, 49, 3187.
48. Pavlidou, S.; Papaspyrides, C. D. Prog Polym Sci 2008, 33, 1119.
49. Hirschler, M. M. In Fire and Polymers: Materials and Solutions for Hazard Prevention; Nelson, G. L.; Wilkie, C. A., Eds.; American Chemical Society: Washington, DC, 2001; Chapter 23.
50. Babrauskas, V. In Heat Release in Fires; Babrauskas, V.; Grayson, S. J., Eds.; E & FN Spon: London, 1992; Chapter 2.
51. Hirschler, M. M. In Heat Release in Fires; Babrauskas, V.; Grayson, S. J., Eds.; E & FN Spon: London, 1992; Chapter 12a.
52. Li, B.; Wang, J. J Fire Sci 1997, 15, 341.
53. Li, B. Polym Degrad Stab 2000, 68, 197.
54. Li, B. Polym Degrad Stab 2002, 78, 349.
55. Beyer, G. J Fire Sci 2005, 23, 75.
56. Schartel, B.; Bartholomai, M.; Knoll, U. Polym Degrad Stab 2005, 88, 540.
57. Schartel, B.; Hull, T. R. Fire Mater 2007, 31, 327.
58. Wang, J.; Li, B. Polym Degrad Stab 1999, 63, 279.
59. Li, B.; Wang, J. J Vinyl Addit Techn 2001, 7, 37.
60. Li, B. Polym Degrad Stab 2003, 82, 467.
61. Anderson, R. C.; Scarrott, D.; Keeran, R.; Prest, W.; Carlson, R. F. In Heat Treating: ASM Handbook, 10th ed.; ASM International: Materials Park, OH, 1991; Vol. 4, p 492.